The Behaviour of Neuro-2A Cells on Silicon Substrates with Various Topographies Generated by Femtosecond Laser Micromachining

Sara Mingu[1*][a], Ihor Pavlov[2][b], Çağdaş Devrim Son[1,3][c] and Alpan Bek[1,2][d]

¹Micro and Nanotechnology Graduate Program, Middle East Technical University, 06800, Ankara, Turkey
²Department of Physics, Middle East Technical University, 06800, Ankara, Turkey
³Department of Biological Sciences, Middle East Technical University, 06800, Ankara, Turkey

Abstract: The interaction of neural cells with silicon surfaces is important for basic research as well as for various possible applications, such as silicon-based neural implants and neurochips. Laser structuring of silicon provides a quick and versatile method for the generation of complex, hierarchical topographies on precise locations of the substrate. The behaviour of Neuro-2A cells with laser-structured silicon substrates was studied using a live-imaging setup with fluorescence microscopy. Neuro-2A cells were able to adhere to polished silicon, ripples and microcolumns to different extents, depending on the substrate topography and incubation time. Initially, cells adhere much better to structured areas, resulting in visible cell patterning on the substrates. Time-lapse microscopy revealed cell exploration and motility behaviours on the substrates. Cell motility was significantly decreased on structured substrates, with whole area microcolumns having the slowest cell motility. On polished silicon, cells were found to interact with the substrates using lamellipodia and filopodia. After 24 or 48 hours, cells were better able to adhere to polished as well as structured silicon. Neurite alignment was observed on microcolumn and trench substrates. On the other hand, highly processed substrates were inhibitory to cell growth and resulted in poor cell health.

1   INTRODUCTION

The interaction of cells with their physical environment, including substrate topography, is important in basic and applied research in tissue engineering and regenerative medicine. Cells have been shown to respond to substrates via alterations in adhesion, proliferation, shape or differentiation state (Dalby, 2014; Yang, 2015).

As a general rule, it is believed that specific parts of the cells interact with topographical features of similar size: small sized features (tens of nm) interact with integrins, micron-sized features interact with focal adhesions, while larger topographical features (tens of microns) may interact with the cell bodies. In particular, neurites were found to interact with topographical features of various sizes (Yim, 2016). The underlying biochemical mechanisms have not been completely elucidated, and there is ongoing research on the interaction of cells with substrates. The parameters to consider are the choice of substrate materials, the micromachining methods, the substrate surface topographies, and the cell types.

Different materials such as polymers, glass, steel, gold, platinum, titanium and silicon have been shown to be appropriate cell substrate materials, and various modification techniques have been characterized (Mendes, 2013). Out of these, silicon has extensively been studied as a cell substrate, also due to its importance in microelectronics. It is possible to generate different topographies on silicon with lithographic or chemical etching techniques. Silicon has been proposed as a base material for implantable electronic devices and has been shown to be biocompatible in vivo in various forms: bare, coated with chemicals such as poly-lysine, as well as in forms of porous silicon, quartz, and fused silica

[a] https://orcid.org/0000-0002-7332-0764
[b] https://orcid.org/0000-0001-9494-4149
[c] https://orcid.org/0000-0002-4076-5441
[d] https://orcid.org/0000-0002-0190-7945

(Khan, 2010). Silicon has been previously studied as a biomaterial with various cell types.

Direct laser writing is a fast, one-step procedure; it does not require masks or other treatments, it can be performed in air, and can be used to structure silicon (Guo, 2013). Laser processing in silicon generates complex hierarchical morphologies, which have features in both micro- and nanoscale and thus resemble in-vivo topographies. A wide variety of structures is possible simply by changing the laser fluence. These include channels/trenches, micro-columns covered in nano-roughness, as well as laser-induced periodic surface structures (LIPSS). In particular, LIPSS may be of two types, high spatial frequency (HSFL), having a period smaller than the wavelength of the laser, or low spatial frequency (LSFL), having a period close to the wavelength. In our study, LSFL LIPSS is used; to the best of our knowledge, no other study reports the interaction of LSFL LIPSS on silicon with cells. Femtosecond-laser induced LIPSS is interesting because it is a regular grating-like structure covered in nano-roughness. As such, it may resemble ordered fibres in the cells' natural environment. Many studies try to replicate ordered fibres by polymer electrospinning or lithographic techniques. However, with laser, unlike other procedures, selective processing of defined areas on a single substrate and in a single step is possible, allowing for simultaneous comparison of different topographies on the same substrate without any mask.

Neural cells are particularly important, due to possible applications for neural prosthetics or chips. As such, there has been extensive research on the interaction of various primary neurons or neural stem cell lines with topographies on different materials (Simitzi, 2018). In the present study, the Neuro-2A cell line was chosen, as a fast-growing, widely available cell line which can differentiate into neural cells spontaneously or upon induction. Neuro-2A cells have previously been used in studies of cell-substrate interactions. In one study, Neuro-2A cell adhesion and localization was modulated on PDMS chips subjected to chemical treatments, and communicating neural networks were formed (Yaghoub, 2005). In another study, 20 micron-width grooves on PDMS were found to be optimal for cell density, neurite alignment and differentiation rate for Neuro-2A cells (Beduer, 2011). Neuro-2A cells have also been previously studied on silicon substrates. It was shown that Neuro-2A cells prefer porous silicon of pore sizes 8 to 75 nm compared to flat silicon, and that the cell clustering was changed on the porous

surfaces, possibly forming neural networks (Gentile, 2016).

In this work, Neuro-2A cells were observed interacting with various topographies on silicon including ablation based microcolumns and LIPSS based nanoscale ripples using time-lapse microscopy and confocal microscopy. To our knowledge, this is the first study where this cell line is used on laser structured silicon substrates, including LIPSS topographies, using live imaging.

2 METHODS

2.1 Laser Structuring of Silicon Substrates

Single-side polished, p-type silicon substrates were cut into 0.5 mm or 16 mm side squares using precise laser cutting, in order to ensure an equal number of cells seeded onto each substrate. The surfaces were cleaned with hydrogen fluoride for five minutes before the laser processing. The Laser Induced Periodic Surface Structures and other topographies were created using our home-made ultrafast laser system with central wavelength at 1030 nm, pulse duration of 370 fs, repetition rate of 1 MHz, and with up to 1 W of average power. The focused beam spot size was 9 μm. The system was equipped with a waveplate for controlling polarization of the laser beam on the sample, a 3D motorized stage, as well as precision motion stages. The laser beam was be raster-scanned onto the substrate using various shapes, velocities and hatch values (distance between raster-scan lines). The laser processing was carried out in air. On 5 mm square substrates, 3mm square patterning was done. On the 16 mm square substrates, 12 rectangles of 3 mm x 2.5 mm were structured, of 4 different topographies with 3 replicas, each.

2.2 Substrate Cleaning and Characterization

Laser-structured silicon substrates were cleaned using 3 solvents (acetone, absolute ethanol and isopropanol) for 10 minutes each in an ultrasonic bath, dried using nitrogen air flow, and stored in a closed container until characterization or use. Topographies were characterized using Scanning Electron Microscopy (Zeiss).

2.3 Cell Culture

Neuroblastoma cells were purchased from ATCC (Neuro-2A line, albino mouse origin, ATCC® CCL-131™) and maintained in complete medium containing Dulbecco's Modified Eagle Medium (DMEM) and reduced serum medium (OptiMEM), supplemented with 10% Fetal Bovine Serum (FBS) and 1% Penicillin/Streptomycin. For differentiation purposes, cell medium containing 1% FBS was prepared. The cells were incubated in 37°C and 5% CO2 in a Nüve EC 160 incubator. During routine splitting procedures, the cells were washed using Phosphate Buffered Saline (PBS) and detached using TrypLE dissociation reagent. 24 hours prior to cell seeding, the cells were transiently transfected with fluorescent protein constructs using Lipofectamine LTX. The DNA constructs included membrane-bound or nucleus-localized EGFP constructs equipped with the appropriate localization signals (Gap-43 signal for membrane and c-myc NLS for nucleus, respectively). The DNA constructs were generated using standard molecular cloning procedures. The Gap43 signal sequence was MLCCMRRTKQVEKNDEDQKI, while the NLS sequence was PAAKRVKLD. The amount of transfected plasmid was 500 ng in all cases. All cell culture experiments were carried out in a laminar flow hood equipped with HEPA filter to ensure sterile conditions.

2.4 Cell Seeding on the Silicon Substrates

The silicon substrates were sterilized by immersion in 70% ethanol, and then immersed in complete cell medium for 10 minutes prior to cell seeding in order to enhance cell adhesion. The cell number was 4000 cells/cm^2 for long duration experiments and 20.000 cells/cm^2 for shorter duration ones. For live imaging experiments, the substrates were placed upside down over confocal glass bottom cell culture dishes. The imaging was done 24 or 48 hours after seeding for pictures; and for a duration of 3 to 24 hours after seeding for live-imaging experiments.

2.5 Cell Imaging and Analysis

The cells were imaged with an inverted fluorescence microscope (Leica) equipped with a confocal setup (Andor) and the appropriate excitation and emission filters for EGFP. The silicon substrates were washed once with HHBS buffer and placed upside down onto a coverslip. For live imaging, the dish containing the silicon sample was placed into a live-imaging chamber equipped with 37°C incubation and 5% CO$_2$ pump to ensure proper cell growth conditions. Images were taken every 2 or 2.5 minutes with 10X objective to observe cell movement on the substrate. All cell image analyses were carried out with ImageJ or FIJI software. Cell motility analysis was carried out using the Manual Tracking Plugin in ImageJ. At least 7 cells were chosen at random and tracked from time-lapse videos of cells on flat, LIPSS and microcolumn topographies. The velocity and distance values were compared for each topography using t-test.

3 RESULTS AND DISCUSSION

The topographies generated on silicon were dependent on the scan velocity of the beam (which in turn controls effective fluence) and the distance between the raster scan lines (hatch). A velocity of 10 mm/s generated deep trench-like topographies with depth of more than 1 μm (Figure 1). In the presented substrate, the distance between the lines is 0.03 mm. A velocity of 100 mm/s generated microcolumn-like line topographies, while velocities larger than 1000 mm/s generated regular ripples (in LIPSS regime). The ripples have depths of 300 nm, periods of 900-1000 μm, and are covered in nano-scale roughness.
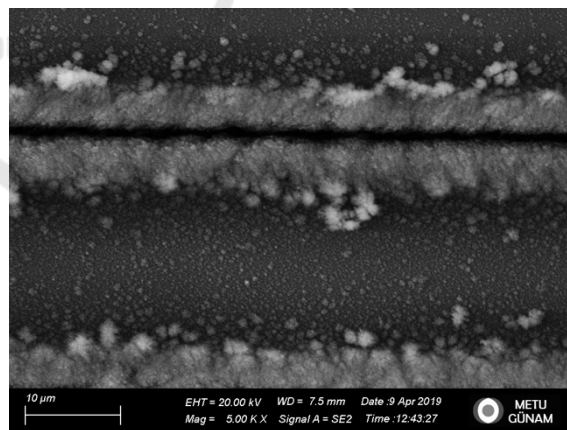

Figure 1: SEM of trench topography generated with a single laser pass with velocity 10 mm/s, hatch = 0.03 mm, 5.000X magnification.

Figure 2 shows a combination of the LIPSS with microcolumn topography, generated by scanning 100 mm/s lines over LIPSS topography. LSFL type LIPSS topography was generated by raster scanning over the whole area with velocity 1500 mm/s and hatch value of 0.005 mm (Figures 2 and 3). The direction of the ripples depends on the polarization of

the beam. Finally, whole-area microcolumn topographies were generated by raster-scanning the beam at 100 mm/s using a hatch value of 0.005 mm. The resulting topography is shown in Figure 4. Structured silicon substrates of square shape and 1.6 cm side length are shown in Figure 5. Neuro-2A cells showed different adhesion and motility on the various substrates. The cell response was highly dependent on the initial cell density, presence of clumps, serum amount in the cell medium, and number of hours of incubation.
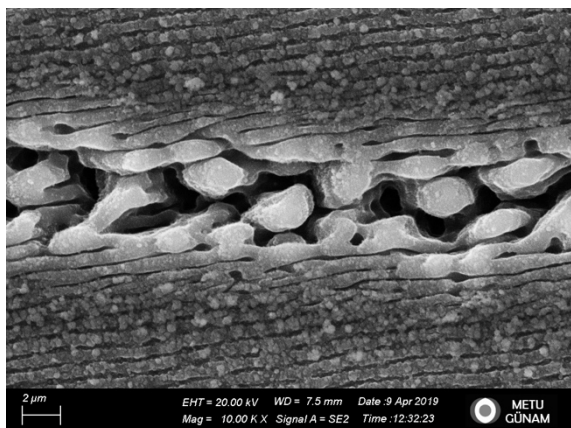
Figure 2: SEM of microcolumn line topography on LIPSS, generated with velocity 100 mm/s, hatch = 0.03 mm, overlaid on velocity 2000 mm/s, hatch = 0.005 mm, 10.000X magnification.
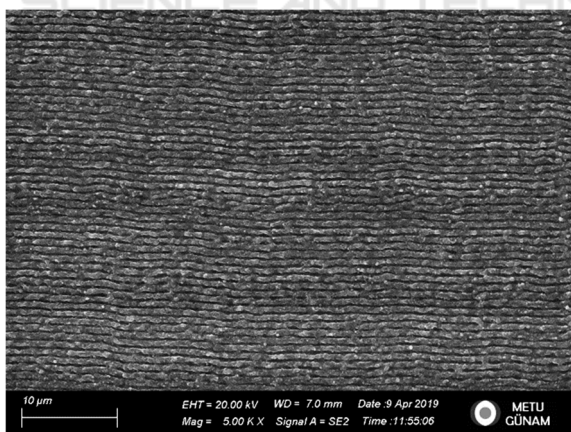

Figure 3: SEM of LIPSS topography generated with velocity 2000 mm/s and hatch = 0.005 mm, 5.000X magnification.

In general, clumped cells were more likely to keep adhering to each-other through cell-cell adhesions and less likely to differentiate when exposed to low serum media or to respond to the underlying features. This has previously been reported for other cell types (Menzies KL., 2010).
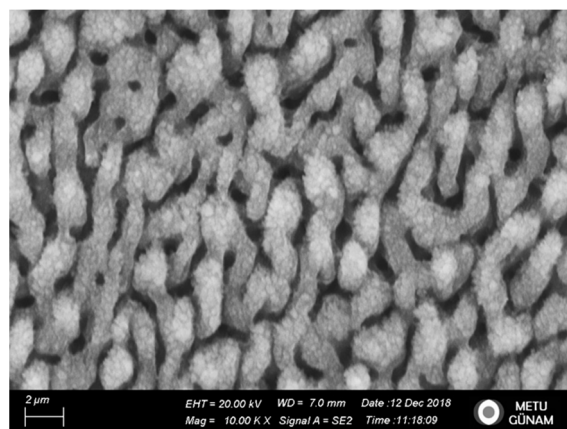

Figure 4: SEM of microcolumn topography generated with velocity 100 mm/s, hatch = 0.005 mm, 10.000X magnification.
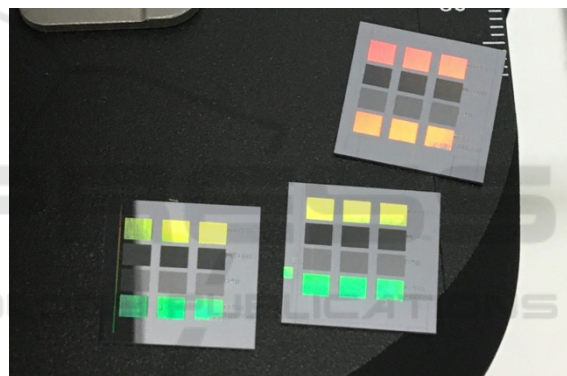

Figure 5: 16 mm square silicon substrates used for experiments. The three substrates are replicas. Each small structured area is 3 mm by 2.5 mm. The first row is LIPSS, as in Figure 3. The second row is microcolumn topography as in figure 4. The third row is trench topography, as in Figure 1. The fourth row is microcolumn line topography on LIPSS, as in figure 2.

One important point is that, although the base material is silicon, the top part of the substrate is expected to be a native layer of silicon oxide, SiO_2, of depth around 10 nm (Fan, 2002). The substrates were not treated with any agents such as HF to remove the top oxide layer. Both Si and SiO_2 were reported to be non-toxic to cells, but also to not support good cell adhesion (Fan, 2002).

In the first few hours, cells showed highly differential adhesion on the polished and structured substrates. At 3 hours, the cell adhesion was weakest on the flat regions, with a very low number of cells staying attached after a single washing step. It is

possible that cell adhesion on structured regions occurs faster, due to the higher surface area of the structured parts. As a result, cell patterning could be achieved on the first few hours of incubation. Cell patterning is shown in Figures 6.
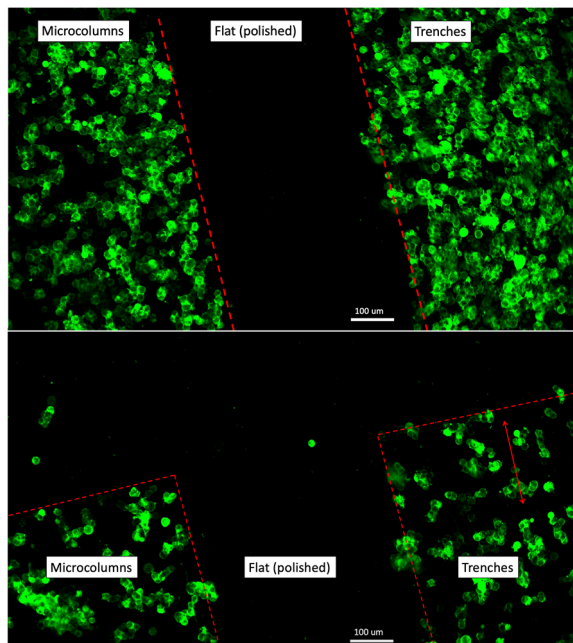

Figure 6: Cell patterning seen on multi-structured substrates shown in Figure 5, after 3-hour incubation. 20.000 cells/cm^2 were seeded on the substrate. Cells were expressing membrane localized EGFP. Top and bottom images are representative edge and vertex regions of the structured squares and were taken on the same substrate.

Similar cell patterning has been shown for nigral cells on etched silicon wafers (Fan, 2002) and for SW10 cells on laser-structured silicon (Yiannakou, 2017). In the latter study, the cells showed a similar positive response to microcolumn-like topographies, while being repelled by ripple topographies of very low periodicity; on the other hand, LSFL LIPSS regime was not considered. In the present study, LSFL LIPSS was not found to have any negative effect on Neuro-2A cell adhesion. The cell patterning here was exclusively due to adhesion differences, since cell migration out of the polished regions could not have occurred at such a short time.

Time-lapse microscopy revealed the cell motility and exploration patterns on the different structured surfaces. Time-lapse recordings of cells on polished silicon, taken 3 hours or 24 hours after seeding showed exploratory behaviour with lamellipodia and filopodia. Two representative cells exploring the polished silicon are shown in Figure 7.
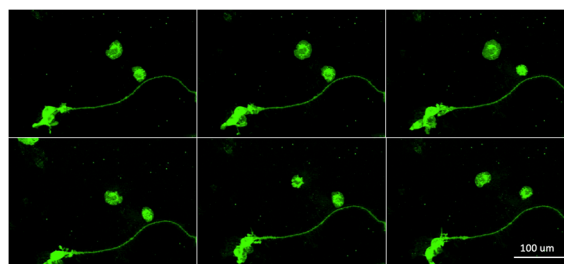

Figure 7: Time-lapse snapshot insets, showing cells moving on polished silicon. The time-lapse was taken with 10X objective. The cells had been transfected with membrane targeted EGFP and had been growing in complete medium for 16 hours followed by 1% FBS medium for 2 hours. Each frame corresponds to 6 minutes.
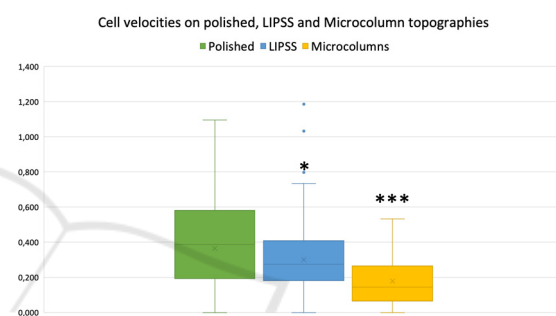

Figure 8: Cell velocities on polished silicon, LIPSS and microcolumn topographies.
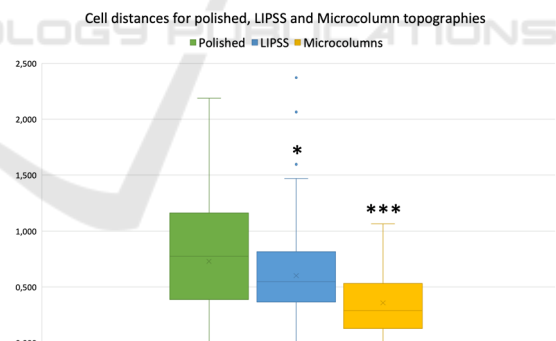

Figure 9: The distances covered by the cells between frames were significantly different on polished silicon, LIPSS and microcolumn topographies.

Cell motility, defined as velocity and distance travelled between frames, was dependent on the underlying topography. Both velocities and distances were found to be significantly different among polished, LIPSS and microcolumn topographies, with cells moving fastest on polished silicon, significantly slower on LIPSS (p<0.5, *) and slowest on microcolumns (p<0.001, ***). Box and whisker plots of velocities and distances travelled by cells on the

different topographies are shown in Figures 8 and 9, respectively.

Cells are observed to move preferentially along the lines back and forth on the topography shown in Figure 2 and extend one or two neurites along the line structures reversibly during movement. The width of the line is around 10 μm (Figure 2), about half the size of the cell soma. Cells confinement to these lines may further reflect the cells' preference to these structures. However, the migration of these cells is faster than that of the cells found in whole area microcolumns (which is evident in live videos), pointing out that it may be the line topography, and possibly the interaction of the thin line of the microcolumns with the underlying LIPSS, which elicits this effect.
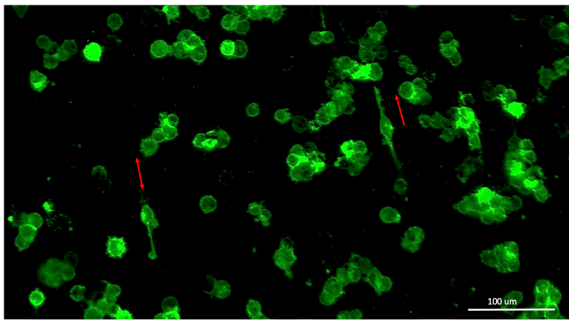

Figure 10: Inset of 10X objective time-lapse recording showing aligned cells on the microcolumn lines on the topography.

The cell response was different after 24 or 48 hours in culture, possibly due to better adhesion on polished silicon, or cell movement on the substrates. More cells remained adhered to polished silicon after 24 or 48 hours, compared to 3 hours.
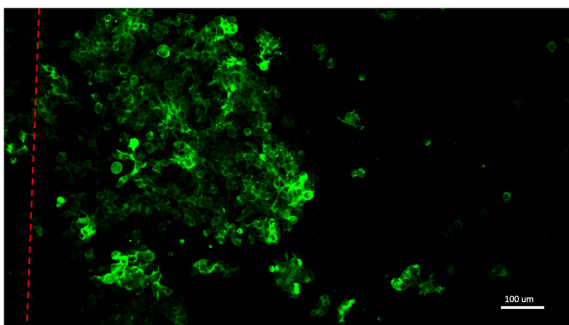

Figure 11: 10X objective image showing cells on LIPSS, expressing membrane localized EGFP. The cells had been growing in complete medium for 24 hours.

When seeded onto line topographies, cells showed neurite alignment to trenches or microcolumns after 24 or 48 hours in culture. Neurite alignment has previously been shown in another study, using ridge-groove substrates generated by multi-step electronic lithographic methods (Johansson, 2006). In the present study, a similar effect may be achieved with a simpler procedure.

On LIPSS, cells were able to remain adhered after 24 or 48 hours. No cell body alignment or elongation was observed. A representative image of cells growing on LIPSS is shown in Figure 11. Images of cells with aligned neurites are shown in Figures 12-15.
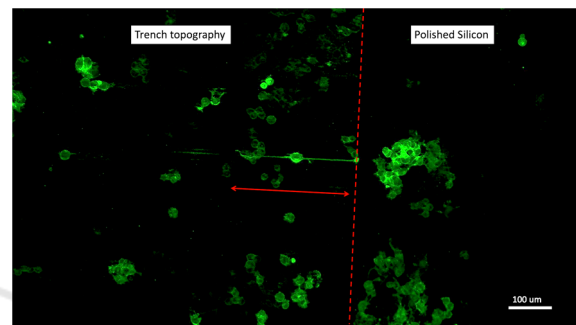

Figure 12: 10X objective image showing various cell clumps as well as differentiated Neuro-2A cell expressing membrane localized EGFP and aligned neurites. The topography consists of trenches, such as in Figure 1. The cells had been growing in 1% serum medium for 48 hours.
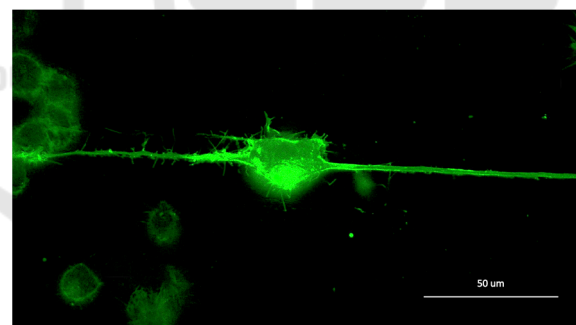

Figure 13: Confocal 63X oil immersion objective image of the cell shown in Figure 12. The neurites are on the trenches.

On the other hand, cell body alignment was not observed for any of the substrates, except for during cell movement on trenches and microcolumn lines, as seen in time-lapse videos. Cells which were found moving on the lines or trenches tended to have a more elliptical shape compared to the other cells, with the longer axis coinciding with the topography lines. However, the shape of the cells was dynamic throughout the time-lapse imaging.

The cells did not respond well to substrates which were highly processed. A representative image is
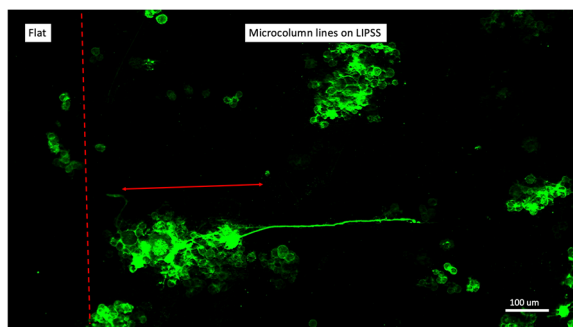
Figure 14: 10X objective image showing various cell clumps as well as differentiated Neuro-2A cell expressing membrane-localized EGFP and aligned neurites. The cells had been growing in 1% serum medium for 24 hours. The topography consists of microcolumn lines on LIPSS, the red arrow shows the direction of the microcolumn lines and LIPSS.
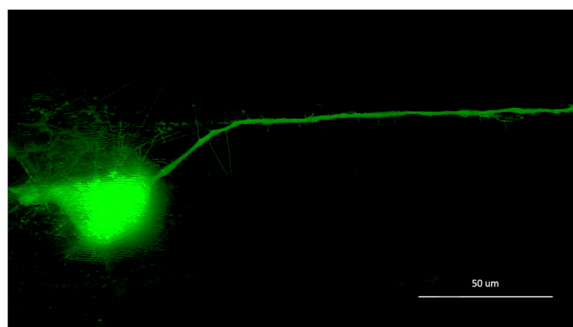

Figure 15: 63X oil immersion objective image of the cell shown in Figure 14. The neurite extended onto the microcolumn line. The LIPSS topography can be seen under the cell body.
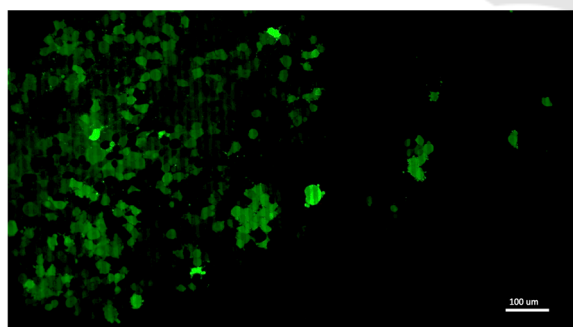

Figure 16: 10X magnification image showing blebbing behaviour of Neuro-2A cells on substrates on highly processed substrates. The cells had been growing for 24 hours in complete medium and express nuclear-localized EGFP. The substrate consists of trenches like in Figure 1, with hatch value of 20 μm.

shown in Figure 16. In these cells, nuclear localization fluorescent proteins were found throughout the cell, suggesting that the nuclear

integrity was compromised. Moreover, the cells display blebbing behaviour. This suggests that it could be possible to make regions which are cell-inhibitory in over longer incubation periods, simply by excessive laser damage.

4 CONCLUSIONS AND FUTURE WORK

The behaviour of Neuro-2A cells was observed on different time points on polished and laser-structured silicon, using confocal fluorescence and time-lapse microscopy. The cells displayed different behaviours depending on the topography and incubation time. At short incubation times, cells were more likely to attach to the structured areas, opening up the possibility for easy cell patterning. At later times, the cell adhesion on all structures was improved, and neurite alignment effects were observed.

Similar to the cell adhesion, also motility on the substrates was affected by the underlying topographies. Further work may include studying the behaviour of different proteins using live imaging setups in silicon and other opaque materials, for example actin dynamics and stress fibre formation on the different topographies.

Finally, future work may include live observation of protein-protein interactions on different substrates with methods such as FRET, which may be valuable to understand the biochemical mechanisms underlying the wide variety of cell responses on topographies.

REFERENCES

Beduer, A., Vaysse, L., Flahaut, E., Seichepine, F., Vieu, C., 2011. Multi-scale engineering for neuronal cell growth and differentiation. *Microelectron. Eng.* 88, 1668-1671.

Dalby, M., Gadegaard, N., Oreffo, R., 2014. Harnessing nanotopography and integrin-matrix interactions to influence stem cell fate. *Nat. Mater.* 13, 558-569.

Fan, Y.W., Cui, F.Z., Hou, S.P., Xu, Q.Y., Chen, L.N., Lee, I.S., 2002. Culture of neural cells on silicon wafers with nano-scale surface topography. *J. Neurosci. Meth.* 120, 17-23.

Gentile, F., Marinaro, G., Rocca, R., Berberio, M., Cancedda, L., Di Fabrizio, E., Decuzzi, P., 2015. Networks of neuroblastoma cells on porous silicon substrates reveal a small world topology. *Integr. Biol.* 7(2),184–197.

Guo, C., Vorobyev, A., 2013. Direct femtosecond laser surface nano/microstructuring and its applications. *Laser Photonics Rev.* 7(3), 385-407.

Johansson, F., Carlberg, P., Danielsen, N., Montelius, L., Kanje, M., 2006. Axonal outgrowth on nano-imprinted patterns. *Biomaterials* 27, 1251-1258.

Khan, S., Newaz, G., 2010. A comprehensive review of surface modification for neural cell adhesion and patterning. *J. Biomed. Mater. Res.* 93A(3) 1209-1224.

Mendes, P.M., 2013. Cellular nanotechnology: making biological interfaces smarter. *Chem. Soc. Rev.* 42, 9270.

Menzies, K.L., Jones, L., 2010. The impact of contact angle on the biocompatibility of biomaterials. *Optom. Vis. Sci.* 87, 387.

Simitzi, C., Stratakis, E., Karali, K., Ranella, A. 2018. Controlling the outgrowth and functions of neural stem cells: the effect of surface topography. *ChemPhysChem* 19(10), 1143-1163.

Yaghoub, M., Tremblay, R., Voicu, R., Mealing, G., Monette, R., Py, C., Faid, K., Sikorska, M. 2005. Neurogenesis and neuronal communication on micropatterned neurochips. *Biotechnol. Bioeng.* 92(3), 336-345.

Yang, L., Liu, H., Yin, Y. 2015. Biomaterial nanotopography-mediated cell responses: experiment and modeling. *International Journal of Smart and Nano Materials* 5(4), 227-256.

Yiannakou, C., Simitzi, C., Manousaki A., Fotakis C., Ranella A., Stratakis E. 2017. Cell patterning via laser micro/nano structured silicon surfaces. *Biofabrication* 9, 025024.

Yim, E.N., 2016. From nano to micro: topographical scale and its impact on cell adhesion, morphology and contact guidance. *J. Phys.: Condens. Matter.* 28, 183001.